Bull. Soc. R. Sci. Liège, 2024, **93**(2), 797–810 *Peer-reviewed conference paper*
doi:10.25518/0037-9565.11883

Spectroscopic and Photometric Study of the Low-luminous AGN NGC 4395

Shivangi PANDEY[1,2,*], Suvendu RAKSHIT[1], Priyanka JALAN[1,3] and Krishan CHAND[1,4]

[1] Aryabhatta Research Institute of Observational Sciences, Nainital–263001, Uttarakhand, India
[2] Department of Applied Physics, Mahatma Jyotiba Phule Rohilkhand University, Bareilly–243006, India
[3] Center for Theoretical Physics of the Polish Academy of Sciences, Al. Lotników 32/46, 02-668 Warsaw, Poland
[4] Now at: Department of Physics and Astronomical Science, Central University of Himachal Pradesh, Dharamshala, Kangra–176215, Himachal Pradesh, India
[*] Corresponding author: Shivangipandey@aries.res.in

Paper presented at the 3rd BINA Workshop on "Scientific Potential of the Indo-Belgian Cooperation", held at the Graphic Era Hill University, Bhimtal (India), 22nd–24th March 2023.

Abstract

The study of intermediate mass black holes (IMBHs) and estimating the black hole mass could potentially elucidate the origin of supermassive black hole (SMBH) seeds present at high redshifts and how they co-evolve with their host galaxy. The difficulty in detecting these IMBHs and the requirement of high spatial resolution to measure BHs mass makes this task challenging. In this work, we have performed photometric and spectroscopic analyses of an extremely low luminosity Seyfert 1 galaxy NGC 4395. Our observations revealed strong emission lines in the spectra, and we observed a fractional variability in the V-band of 12%. Utilizing the broad-line region (BLR) size-luminosity relation for active galactic nuclei (AGNs), we estimated the size of the BLR to be 74 ± 14 light minutes, based on a continuum luminosity of $10^{38}\,\mathrm{erg\,s^{-1}}$ at 5100 Å. Additionally, the gas clouds are found to be revolving with a velocity dispersion of $384\,\mathrm{km\,s^{-1}}$ around the central engine, leading to a black hole mass estimation of $\sim 3.87^{+1.1}_{-1.1} \times 10^5\,M_\odot$.

Keywords: active galaxies, NGC 4395, intermediate-mass black holes, spectroscopy

1. Introduction

Every massive galaxy hosts a supermassive black hole (SMBH) at its core (e.g., Kormendy and Richstone, 1995; Kormendy and Ho, 2013). Active galactic nuclei (AGNs) are powered by the accretion of matter onto the central supermassive black hole, which is surrounded by an accretion disk. A broad-line region (BLR) emits broad lines due to Doppler broadening of high-velocity clouds in BLR (Urry and Padovani, 1995) surrounding the accretion disk.

Therefore, two important aspects have to be addressed. Firstly, the origin of these SMBHs seeds, located at high redshifts (e.g., Mortlock et al., 2011), is believed to be heavier than stellar mass black holes ranging from approximately 10 to $100\,M_{\odot}$. Hence, their progenitors are suggested to be intermediate-mass black holes (IMBH) with masses of 10^3–$10^6\,M_{\odot}$, making them currently active research subjects (e.g., Loeb and Rasio, 1994; Latif et al., 2013; Greene et al., 2020). However, the detection of IMBHs is challenging, mainly due to their low luminosity and negligible variability (see Mezcua, 2017; Greene et al., 2020), and very few candidates have been identified so far (e.g., Greene and Ho, 2004, 2007; Reines et al., 2013).

Secondly, due to the correlation between the black hole masses and the stellar velocity dispersion $\sigma_{\star}$ of the bulge of the galaxy (see, Hu, 2008; Woo et al., 2015), we can gain insight into the mass distribution and co-evolution of supermassive black holes and their host galaxies (Kormendy and Ho, 2013). This requires more accurate measurements of the masses of these IMBHs. However, the spatial resolution needed to observe them exceeds the capability of modern instruments. Hence, most studies of the central engine rely on reverberation mapping (RM; Blandford and McKee, 1982). RM examines the size and structure of the BLR by observing the response of emission lines to continuum variations from the central source and has been applied to more than 100 objects so far (e.g., Blandford and McKee, 1982; Peterson, 1993; Peterson et al., 1998; Kaspi et al., 2000, 2007; Peterson et al., 2002, 2004, 2014; Dietrich et al., 2012; Du et al., 2014, 2015; Woo et al., 2015; Pei et al., 2017; Fausnaugh et al., 2017; Rakshit et al., 2019; Bontà et al., 2020; Williams et al., 2020; Amorim et al., 2021; Cackett et al., 2021; Pandey et al., 2022). The black hole mass, $M_{\rm BH}$, can be estimated via the virial relation from

$$M_{\rm BH} = \frac{f \times R_{\rm BLR} \times \Delta V^2}{G}, \tag{1}$$

where f is the virial factor, which accounts for the kinematics and the geometry of the BLR gas cloud, $R_{\rm BLR}$ is the BLR's size, estimated from the lag τ via $R_{\rm BLR} = c\tau$, and ΔV is derived from the line dispersion or the Full Width at Half Maximum (FWHM).

In this work, we selected an intermediate black hole candidate, located in NGC 4395 (Filippenko and Sargent, 1989), which is a low-luminosity Seyfert 1 galaxy exhibiting strong emission lines at a redshift of 0.001. It hosts the least luminous broad-lined AGN known to date, with a bolometric luminosity lower than $10^{41}\,{\rm erg\,s^{-1}}$ and a stellar mass of approximately $10^9\,M_{\odot}$ (Filippenko and Sargent, 1989; Filippenko and Ho, 2003; Cho et al., 2021). The Eddington ratio of NGC 4395 is $\sim 5\%$ (Woo et al., 2019), which is comparable to that of other reverberation-mapped AGNs. Therefore, this galaxy offers a unique opportunity to investigate photoionization and size-luminosity relations within the extreme low-luminosity regime of AGNs. The exact mass of NGC 4395 is uncertain, with estimates ranging from $9 \times 10^3\,M_{\odot}$ to $4 \times 10^5\,M_{\odot}$ (e.g., Filippenko and Ho, 2003; Peterson et al., 2005; Edri et al., 2012; Woo et al., 2019). We conducted a photometric and spectroscopic study to more accurately determine the black hole mass. Section 2 outlines the photometric and spectroscopic data and the reduction process. Finally, Sect. 3 discusses the preliminary results and future prospects.

Table 1: Photometric observations in the mentioned filters using the 1-m ST and 1.3-m DFOT (*top*) and spectroscopic observations with ADFOSC using the 3.6-m DOT (*bottom*) on 10 and 11 March 2022.

Photometric observations			
Telescopes	**Day**	***V*-band**	***B*-band**
1-m ST	10/03/2022	34	17
	11/03/2022	66	34
1.3-m DFOT	10/03/2022	19	–
	11/03/2022	23	–

Spectroscopic observations		
Telescopes	**Day**	**ADFOSC**
3.6-m DOT	10/03/2022	43
	11/03/2022	64

2. Observation and Reduction

We observed the source using all three telescopes hosted by Aryabhatta Research Institute of Observational Sciences, Nainital, India (ARIES) from 10–11 March 2022, spanning observations for about 7–8 h each night, i.e., several times the expected lag of the source. Photometric observations were performed using the 1.04-m Sampuranand Telescope (ST; Sagar, 1999) in the Johnson–Cousins V and B bands, and the 1.3-m Devasthal Fast Optical Telescope (DFOT; Sagar et al., 2011) in the V band. Spectroscopy of the source was carried out using the 3.6-m Devasthal Optical Telescope (DOT; Kumar et al., 2018). The 4K $\times$ 4K CCD ($0.23''$ per pixel) was used with a 2×2 binning for 1.04-m ST, while the ANDOR 2K $\times$ 2K CCD ($0.53''$ per pixel) was used for undertaking observation with 1.3-m DFOT without binning. Spectroscopic observations were conducted using the ARIES-Devasthal Faint Object Spectrograph and Camera (ADFOSC; Omar et al., 2019) mounted at 3.6-m DOT. It consists of a 4K $\times$ 4K deep-depletion CCD with a $0.2''$ per pixel scale and 2×2 binning. The number of photometric data points and spectra obtained from all these telescopes are reported in Table 1. We obtained 100 and 42 photometric data points from the 1-m ST and the 1.3-m DFOT, respectively, in the V-band, along with approximately 100 spectra from the 3.6-m DOT. These datasets are ideal for lag measurements using various methods and reverberation mapping studies.

2.1. Differential photometry

NGC 4395 is an extended spiral galaxy. It is depicted in Fig. 1, with its core highlighted by a yellow circle, alongside three steady comparison stars marked with green circles. These comparison stars are used for conducting differential photometry. The preprocessing involves cleaning the photometric frames. Aperture photometry (see, Stetson, 1987) is performed using

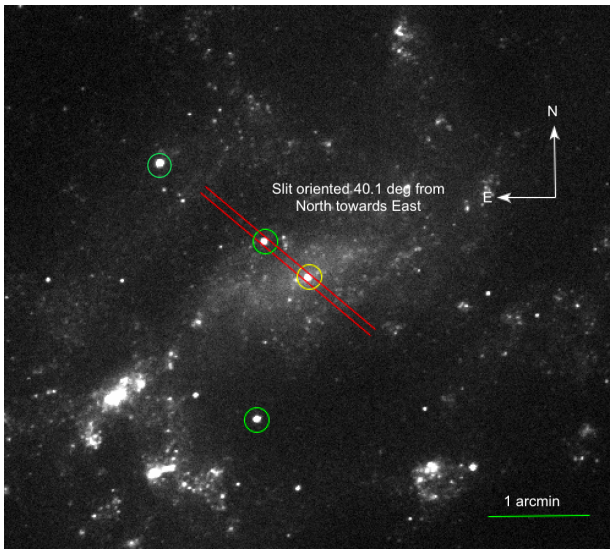

Figure 1: SDSS *g*-band image of NGC 4395. Three comparison stars are marked with green circles, while the target AGN is denoted with a yellow circle. The slit is oriented to cover both the AGN and a comparison star.

the Dominion Astronomical Observatory Photometry II (DAOPHOT II) package. We selected the aperture size to be twice the FWHM of the point spread function (PSF) or seeing. The differential magnitude of the source was calculated with respect to three comparison stars present within the same field. The light curve obtained from the 1.3-m DFOT on both days is shown in Fig. 2; the first three panels show the differential variation of the AGN with respect to each comparison star, whereas the last three panels show the differential variations between the stars themselves. This enables the detection of AGN variation in comparison to the steady comparison stars..

2.2. Spectroscopic reduction and analysis

For spectroscopy with the 3.6-m DOT, we used ADFOSC with a 3.2 arcsec wide and 8 arcsec long slit, along with a 132R600 gr/mm grism covering the wavelength range from 3500 to 7000 Å centred at 4880 Å. Spectroscopic frames with a duration of 300 s each were acquired throughout the night, along with bias and flat frames for preprocessing. Preprocessing includes bias subtraction, flat fielding, and cosmic ray removal with the L. A. cosmic algorithm (Dokkum, 2001). Additionally, observations of the HgAr lamp were conducted in the same configuration to provide a wavelength solution. The reduction was carried out with IRAF (Tody, 1986, 1993; National Optical Astronomy Observatories, 1999).

Given that the source is extended, resolved, and low luminous, detecting its variability poses a significant challenge, primarily due to the contribution of the host galaxy (see, Cho et al., 2021). Therefore, achieving accurate flux calibration relative to a reference star was essential, the more since the narrow-line flux was also found to be variable. To address this, we oriented the slit so that it covered a nearby comparison star, as illustrated in Fig. 1. This

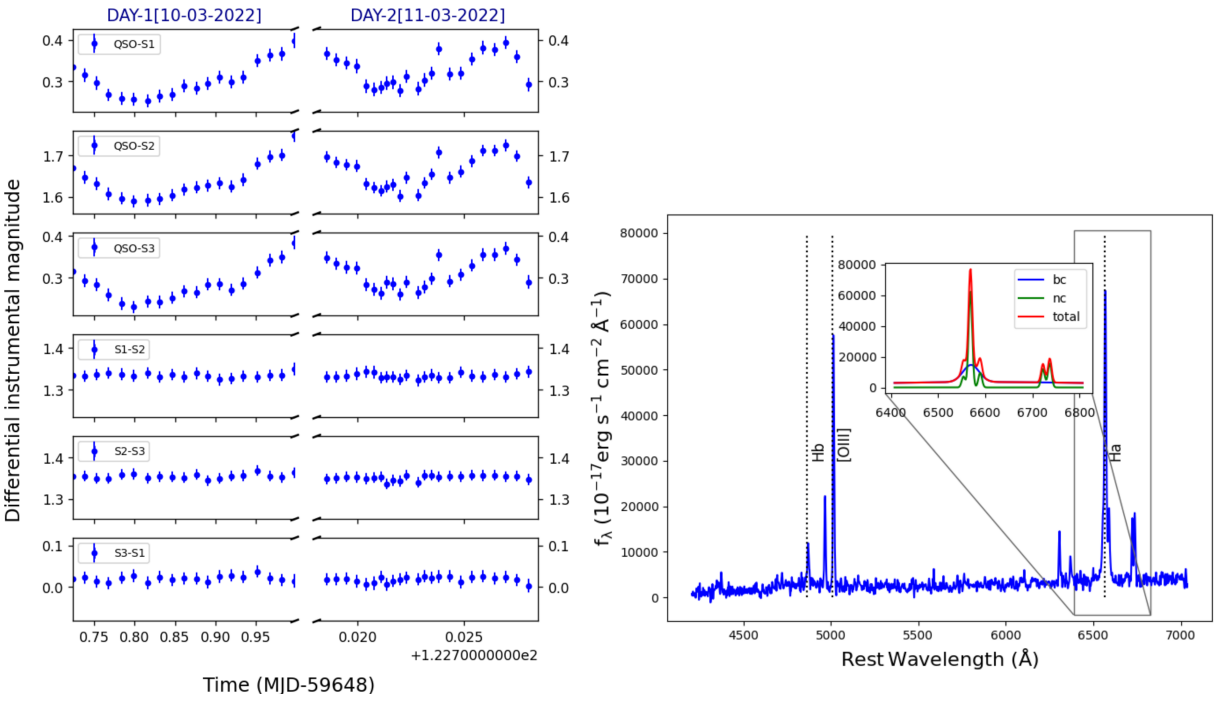

Figure 2: (*Left*) The differential photometric light curve of NGC 4395 on 10–11 March 2022 ($l - r$) is shown in the V band taken from the 1.3-m DFOT. The upper three panels depict the differential magnitudes of the AGN relative to each star; he lower three panels show the variation among each comparison star. (*Right*) One of the spectra from 10 March 2022, fitted with PyQSOfit. The main plot shows the spectrum with marked emission lines. The inset panel shows the decomposition of the Hα component into narrow and broad components.

arrangement makes it possible to acquire simultaneous spectra for both the source and a steady comparison star.

For decomposition and spectrum fitting, we called upon the publicly available multicomponent spectral fitting code PyQSOfit (Guo et al., 2018). A detailed description of the code and of its applications can be found in Guo et al. (2019), Shen et al. (2019) and Rakshit et al. (2020). Each spectrum was corrected for Galactic extinction using the Schlegel et al. (1998) map and the Milky Way extinction law of Fitzpatrick (1999) with $R_V = 3.1$. Subsequently, we de-redshifted it using the redshift. Following this, the continuum was modelled using power-law and Fe II templates. After subtracting the continuum, detailed multi-Gaussian modelling was performed in the Hα region to fit the emission lines. The narrow Hα, NII6549, NII6585, SII6718, and SII6732 lines were modelled using a single Gaussian with the velocity and velocity offset tied to each other. The broad Hα component was modelled with double Gaussians. The best-fit model was obtained via χ^2 minimization. From the fitting, we then calculated the emission line flux and width, and the continuum luminosity at 5100 Å.

Figure 2 shows an example of spectral fitting with PyQSOfit, where various emission lines are marked, including broad and narrow emission line components. Detailed emission line flux

calibration, based on the reference star, is required to construct the emission line light curve and perform cross-correlation.

3. Discussion and Future Prospects

3.1. Preliminary results

We observed strong emission lines in the spectra of NGC 4395, including a broad Hα line. The fractional variability in the V-band was found to be 12%. Using the flux at 5100 Å, we estimated the continuum luminosity at the same wavelength to be $10^{38}\,\mathrm{erg\,s^{-1}}$. Moreover, employing the single-epoch BLR size-luminosity relation provided by Cho et al. (2023) based on Hα, we estimated the BLR size to be 74 ± 14 light minutes. Using Eq. (1), the Hα BLR size, the second moment (σ_{line}) of the Hα emission line from the single epoch spectrum, and adopting a value of 4.47 for the virial factor f (Woo et al., 2015), we calculated the virial mass of the black hole to be $3.87^{+1.1}_{-1.1} \times 10^5\,M_\odot$, taking into account the uncertainty of virial factor (i.e., $\sigma(\log_{10} f) = 0.12$; Woo et al. (2015)). The virial coefficients for different Balmer lines are approximately the same, as supported by extensive studies on multiple emission lines for individual sources (e.g., Williams et al., 2020; Williams et al., 2021). Therefore, we adopted virial factor values obtained by Woo et al. (2015) based on Hβ. To estimate the uncertainty in the line width measurements and, consequently, the black hole mass, we employed the Monte Carlo bootstrap method (Peterson et al., 2004). Within the initially selected Hα region (i.e., 6590–6610 Å), we randomly varied the endpoints by ± 10 Å. This process was repeated for a total of 5000 realizations, generating distributions of FWHM and σ_{line}. The mean of these distributions represented the final line width, while the standard deviation (calculated as the 34$^{\mathrm{th}}$ percentile on both sides of the mean, i.e., the 16$^{\mathrm{th}}$ and 84$^{\mathrm{th}}$ percentiles of the distribution) served as the measurement uncertainty.

3.2. Future prospects

As mentioned above, accurate flux calibration based on the reference star present in the slit is necessary, as the detected continuum variability is very small (~ 0.1 mag), and the usual narrow-line based flux calibration cannot be performed due to the variability of the resolved narrow-line flux (Cho et al., 2021). Therefore, we plan to do that for individual spectra to obtain a well-calibrated emission line light curve. Additionally, we have photometric light curves in the B and V bands using the 1.3 m DFOT and 1.04 m ST, with a cadence of ~ 5 min. These light curves will be used to compare our spectroscopic continuum light curve at f_{5100} and estimate the lag between the photometric and emission-line light curves. We will conduct cross-correlation analysis (ICCF and DCF) as well as JAVELIN modelling of the light curves to estimate the BLR size (see, Rakshit, 2020; Pandey et al., 2022). This will allow us to accurately estimate the black hole mass of NGC 4395, providing insight into whether the established BLR size-continuum luminosity relation of the SMBHs of AGNs can be extended to active galaxies with luminosities $\ll 10^{41}\,\mathrm{erg\,s^{-1}}$.

Acknowledgments

SR acknowledges the partial support of SERB-DST, New Delhi, for this work through SRG grant no. SRG/2021/001334. The assistance from the scientific and technical staff at the Aryabhatta Research Institute of observational sciencES (ARIES), Nainital, India, is gratefully acknowledged. This work is based in part on observations obtained with the 3.6-m Devasthal Optical Telescope (DOT), the 1.3-m Devasthal Fast Optical Telescope (DFOT) and the 1-m Sampuranand Telescope (ST), all run and managed by ARIES, an autonomous Institute under the Department of Science and Technology, Government of India.

Further Information

Authors' ORCID identifiers

0000-0002-4684-3404 (Shivangi PANDEY)
0000-0002-8377-9667 (Suvendu RAKSHIT)
0000-0002-0524-5328 (Priyanka JALAN)
0000-0002-6789-1624 (Krishan CHAND)

Author contributions

SP and SR designed the project, performed the data reduction and analysis, and wrote the manuscript. SP, KC, and PJ performed the observations.

Conflicts of interest

The authors declare no conflict of interest.

References

Amorim, A., Bauböck, M., Bentz, M. C., Brandner, W., Bolzer, M., Clénet, Y., Davies, R., De Zeeuw, P. T., Dexter, J., Drescher, A., Eckart, A., Eisenhauer, F., Förster Schreiber, N. M., Garcia, P. J., Genzel, R., Gillessen, S., Gratadour, D., Hönig, S., Kaltenbrunner, D., Kishimoto, M., Lacour, S., Lutz, D., Millour, F., Netzer, H., Onken, C. A., Ott, T., Paumard, T., Perraut, K., Perrin, G., Petrucci, P. O., Pfuhl, O., Prieto, M. A., Rouan, D., Shangguan, J., Shimizu, T., Stadler, J., Sternberg, A., Straub, O., Straubmeier, C., Street, R., Sturm, E., Tacconi, L. J., Tristram, K. R., Vermot, P., Von Fellenberg, S., Widmann, F. and Woillez, J. (2021) A geometric distance to the supermassive black hole of NGC 3783. A&A, 654, A85. https://doi.org/10.1051/0004-6361/202141426.

Blandford, R. D. and McKee, C. F. (1982) Reverberation mapping of the emission line regions of Seyfert galaxies and quasars. ApJ, 255, 419–439. https://doi.org/10.1086/159843.

Bontà, E. D., Peterson, B. M., Bentz, M. C., Brandt, W. N., Ciroi, S., Rosa, G. D., Alvarez, G. F., Grier, C. J., Hall, P. B., Hernández Santisteban, J. V., Ho, L. C., Homayouni, Y., Horne, K., Kochanek, C. S., Li, J. I.-H., Morelli, L., Pizzella, A., Pogge, R. W., Schneider, D. P., Shen, Y., Trump, J. R. and Vestergaard, M. (2020) The Sloan Digital Sky Survey Reverberation Mapping Project: Estimating masses of black holes in quasars with single-epoch spectroscopy. ApJ, 903(2), 112. https://doi.org/10.3847/1538-4357/ABBC1C.

Cackett, E. M., Bentz, M. C. and Kara, E. (2021) Reverberation mapping of active galactic nuclei: from X-ray corona to dusty torus. iSci, 24(6), 102557. https://doi.org/10.1016/j.isci.2021.102557.

Cho, H., Woo, J.-H., Treu, T., Williams, P. R., Armen, S. F., Barth, A. J., Bennert, V. N., Cho, W., Filippenko, A. V., Gallo, E., Geum, J., González-Buitrago, D., Gültekin, K., Hodges-Kluck, E., Horst, J. C., Hwang, S. H., Kang, W., Kim, M., Kim, T., Leonard, D. C., Malkan, M. A., Remigio, R. P., Sand, D. J., Shin, J., Son, D., Sung, H.-i. and U, V. (2021) Hα reverberation mapping of the intermediate-mass active galactic nucleus in NGC 4395. ApJ, 921(2), 98. https://doi.org/10.3847/1538-4357/ac1e92.

Cho, H., Woo, J.-H., Wang, S., Son, D., Shin, J., Rakshit, S., Barth, A. J., Bennert, V. N., Gallo, E., Hodges-Kluck, E., Treu, T., Bae, H.-J., Cho, W., Foord, A., Geum, J., Jadhav, Y., Jeon, Y., Kabasares, K. M., Kang, D., Kang, W., Kim, C., Kim, D., Kim, M., Kim, T., N. Le, H. A., Malkan, M. A., Mandal, A. K., Park, D., Park, S., Sung, H.-i., U, V. and Williams, P. R. (2023) The Seoul National University AGN Monitoring Project. IV. Hα reverberation mapping of six AGNs and the Hα size-luminosity relation. ApJ, 953(2), 142. https://doi.org/10.3847/1538-4357/ace1e5.

Dietrich, M., Peterson, B. M., Grier, C. J., Bentz, M. C., Eastman, J., Frank, S., Gonzalez, R., Marshall, J. L., Depoy, D. L. and Prieto, J. L. (2012) Optical monitoring of the broad-line radio galaxy 3C390.3. ApJ, 757(1), 53. https://doi.org/10.1088/0004-637X/757/1/53.

Dokkum, P. G. v. (2001) Cosmic-ray rejection by Laplacian edge detection. PASP, 113, 1420–1427. https://doi.org/10.1086/323894.

Du, P., Hu, C., Lu, K. X., Huang, Y. K., Cheng, C., Qiu, J., Li, Y. R., Zhang, Y. W., Fan, X. L., Bai, J. M., Bian, W. H., Yuan, Y. F., Kaspi, S., Ho, L. C., Netzer, H. and Wang, J. M. (2015) Supermassive black holes with high accretion rates in active galactic nuclei. IV. Hβ time lags and implications for super-Eddington accretion. ApJ, 806(1), 22. https://doi.org/10.1088/0004-637X/806/1/22.

Du, P., Hu, C., Lu, K. X., Wang, F., Qiu, J., Li, Y. R., Bai, J. M., Kaspi, S., Netzer, H. and Wang, J. M. (2014) Supermassive black holes with high accretion rates in active galactic nuclei. I. First results from a new reverberation mapping campaign. ApJ, 782(1), 45. https://doi.org/10.1088/0004-637X/782/1/45.

Edri, H., Rafter, S. E., Chelouche, D., Kaspi, S. and Behar, E. (2012) Broadband photometric reverberation mapping of NGC 4395. ApJ, 756(1), 73. https://doi.org/10.1088/0004-637X/756/1/73.

Fausnaugh, M. M., Grier, C. J., Bentz, M. C., Denney, K. D., Rosa, G. D., Peterson, B. M., Kochanek, C. S., Pogge, R. W., Adams, S. M., Barth, A. J., Beatty, T. G., Bhattacharjee, A., Borman, G. A., Boroson, T. A., Bottorff, M. C., Brown, J. E., Brown, J. S., Brotherton, M. S., Coker, C. T., Crawford, S. M., Croxall, K. V., Eftekharzadeh, S., Eracleous, M., Joner, M. D., Henderson, C. B., Holoien, T. W.-S., Horne, K., Hutchison, T., Kaspi, S., Kim, S., King, A. L., Li, M., Lochhaas, C., Ma, Z., MacInnis, F., Manne-Nicholas, E. R., Mason, M., Montuori, C., Mosquera, A., Mudd, D., Musso, R., Nazarov, S. V., Nguyen, M. L., Okhmat, D. N., Onken, C. A., Ou-Yang, B., Pancoast, A., Pei, L., Penny, M. T., Poleski, R., Rafter, S., Romero-Colmenero, E., Runnoe, J., Sand, D. J., Schimoia, J. S., Sergeev, S. G., Shappee, B. J., Simonian, G. V., Somers, G., Spencer, M., Starkey, D. A., Stevens, D. J., Tayar, J., Treu, T., Valenti, S., Saders, J. V., Villanueva Jr., S., Villforth, C., Weiss, Y., Winkler, H. and Zhu, W. (2017) Reverberation mapping of optical emission lines in five active galaxies. ApJ, 840(2), 97. https://doi.org/10.3847/1538-4357/aa6d52.

Filippenko, A. V. and Ho, L. C. (2003) A low-mass central black hole in the bulgeless Seyfert 1 galaxy NGC 4395. ApJ, 588(1), L13. https://doi.org/10.1086/375361.

Filippenko, A. V. and Sargent, W. L. W. (1989) Discovery of an extremely low luminosity Seyfert 1 nucleus in the dwarf galaxy NGC 4395. ApJ, 342, L11. https://doi.org/10.1086/185472.

Fitzpatrick, E. L. (1999) Correcting for the effects of interstellar extinction. PASP, 111, 63–75. https://doi.org/10.1086/316293.

Greene, J. E. and Ho, L. C. (2004) Active galactic nuclei with candidate intermediate-mass black holes. ApJ, 610, 722–736. https://doi.org/10.1086/421719.

Greene, J. E. and Ho, L. C. (2007) A new sample of low-mass black holes in active galaxies. ApJ, 670, 92–104. https://doi.org/10.1086/522082.

Greene, J. E., Strader, J. and Ho, L. C. (2020) Intermediate-mass black holes. ARA&A, 58, 257–312. https://doi.org/10.1146/annurev-astro-032620-021835.

Guo, H., Liu, X., Shen, Y., Loeb, A., Monroe, T. and Prochaska, J. X. (2019) Constraining sub-parsec binary supermassive black holes in quasars with multi-epoch spectroscopy – III. Candidates from continued radial velocity tests. MNRAS, 482(3), 3288–3307. https://doi.org/10.1093/mnras/sty2920.

Guo, H., Shen, Y. and Wang, S. (2018) PyQSOFit: Python code to fit the spectrum of quasars. Astrophysics Source Code Library, record ascl:1809:008.

Hu, J. (2008) The black hole mass–stellar velocity dispersion correlation: bulges versus pseudo-bulges. MNRAS, 386(4), 2242–2252. https://doi.org/10.1111/j.1365-2966.2008.13195.x.

Kaspi, S., Brandt, W. N., Maoz, D., Netzer, H., Schneider, D. P. and Shemmer, O. (2007) Reverberation mapping of high-luminosity quasars: First results. ApJ, 659(2), 997–1007. https://doi.org/10.1086/512094.

Kaspi, S., Smith, P. S., Netzer, H., Maoz, D., Jannuzi, B. T. and Giveon, U. (2000) Reverberation measurements for 17 quasars and the size-mass-luminosity relations in active galactic nuclei. ApJ, 533(2), 631–649. https://doi.org/10.1086/308704.

Kormendy, J. and Ho, L. C. (2013) Coevolution (or not) of supermassive black holes and host galaxies. ARA&A, 51, 511–653. https://doi.org/10.1146/annurev-astro-082708-101811.

Kormendy, J. and Richstone, D. (1995) Inward bound—The search for supermassive black holes in galactic nuclei. ARA&A, 33, 581–624. https://doi.org/10.1146/annurev.aa.33.090195.003053.

Kumar, B., Omar, A., Maheswar, G., Pandey, A. K., Sagar, R., Uddin, W., Sanwal, B. B., Bangia, T., Kumar, T. S., Yadav, S., Sahu, S., Pant, J., Reddy, B. K., Gupta, A. C., Chand, H., Pandey, J. C., Joshi, M. K., Jaiswar, M., Nanjappa, N., Purushottam, Yadav, R. K. S., Sharma, S., Pandey, S. B., Joshi, S., Joshi, Y. C., Lata, S., Mehdi, B. J., Misra, K. and Singh, M. (2018) 3.6-m Devasthal Optical Telescope project: Completion and first results. BSRSL, 87, 29–41. https://doi.org/10.25518/0037-9565.7454.

Latif, M. A., Schleicher, D. R. G., Schmidt, W. and Niemeyer, J. C. (2013) The characteristic black hole mass resulting from direct collapse in the early Universe. MNRAS, 436(4), 2989–2996. https://doi.org/10.1093/mnras/stt1786.

Loeb, A. and Rasio, F. A. (1994) Collapse of primordial gas clouds and the formation of quasar black holes. ApJ, 432, 52–61. https://doi.org/10.1086/174548.

Mezcua, M. (2017) Observational evidence for intermediate-mass black holes. IJMPD, 26(11), 1730021. https://doi.org/10.1142/S021827181730021X.

Mortlock, D. J., Warren, S. J., Venemans, B. P., Patel, M., Hewett, P. C., McMahon, R. G., Simpson, C., Theuns, T., Gonzáles-Solares, E. A., Adamson, A., Dye, S., Hambly, N. C., Hirst, P., Irwin, M. J., Kuiper, E., Lawrence, A. and Röttgering, H. J. A. (2011) A luminous quasar at a redshift of $z = 7.085$. Natur, 474, 616–619. https://doi.org/10.1038/nature10159.

National Optical Astronomy Observatories (1999) IRAF: Image Reduction and Analysis Facility. Astrophysics Source Code Library, record ascl:9911.002.

Omar, A., Kumar, T. S., Krishna Reddy, B., Pant, J. and Mahto, M. (2019) First-light images from low-dispersion spectrograph-cum-imager on 3.6 m Devasthal Optical Telescope. CSci, 116(9), 1472–1478. https://doi.org/10.18520/cs/v116/i9/1472-1478.

Pandey, S., Rakshit, S., Woo, J.-H. and Stalin, C. S. (2022) Spectroscopic reverberation mapping of Quasar PKS 0736 + 017: broad-line region and black-hole mass. MNRAS, 516(2), 2671–2682. https://doi.org/10.1093/mnras/stac2418.

Pei, L., Fausnaugh, M. M., Barth, A. J., Peterson, B. M., Bentz, M. C., De Rosa, G., Denney, K. D., Goad, M. R., Kochanek, C. S., Korista, K. T., Kriss, G. A., Pogge, R. W., Bennert, V. N., Brotherton, M., Clubb, K. I., Dalla Bontà, E., Filippenko, A. V., Greene, J. E., Grier, C. J., Vestergaard, M., Zheng, W., Adams, S. M., Beatty, T. G., Bigley, A., Brown, J. E., Brown, J. S., Canalizo, G., Comerford, J. M., Coker, C. T., Corsini, E. M., Croft, S., Croxall, K. V., Deason, A. J., Eracleous, M., Fox, O. D., Gates, E. L., Henderson, C. B., Holmbeck, E., Holoien, T. W.-S., Jensen, J. J., Johnson, C. A., Kelly, P. L., Kim, S., King, A., Lau, M. W., Li, M., Lochhaas, C., Ma, Z., Manne-Nicholas, E. R., Mauerhan, J. C., Malkan, M. A., McGurk, R., Morelli, L., Mosquera, A., Mudd, D., Sanchez, F. M., Nguyen, M. L., Ochner, P., Ou-Yang, B., Pancoast, A., Penny, M. T., Pizzella, A., Poleski, R., Runnoe, J., Scott, B., Schimoia, J. S., Shappee, B. J., Shivvers, I., Simonian, G. V., Siviero, A., Somers, G., Stevens, D. J., Strauss, M. A., Tayar, J., Tejos, N., Treu, T., Van Saders, J., Vican, L., Villanueva, S., Yuk, H., Zakamska, N. L., Zhu, W., Anderson, M. D., Arévalo, P., Bazhaw, C., Bisogni, S., Borman, G. A., Bottorff, M. C., Brandt, W. N., Breeveld, A. A., Cackett, E. M., Carini, M. T., Crenshaw, D. M., De Lorenzo-Cáceres, A., Dietrich, M., Edelson, R., Efimova, N. V., Ely, J., Evans, P. A., Ferland, G. J., Flatland, K., Gehrels, N., Geier, S., Gelbord, J. M., Grupe, D., Gupta, A., Hall, P. B., Hicks, S., Horenstein, D., Horne, K., Hutchison, T., Im, M., Joner, M. D., Jones, J., Kaastra, J., Kaspi, S., Kelly, B. C., Kennea, J. A., Kim, M., Kim, S. C., Klimanov, S. A., Lee, J. C., Leonard, D. C., Lira, P., MacInnis, F., Mathur, S., McHardy, I. M., Montouri, C., Musso, R., Nazarov, S. V., Netzer, H., Norris, R. P., Nousek, J. A., Okhmat, D. N., Papadakis, I., Parks, J. R., Pott, J.-U., Rafter, S. E., Rix, H.-W., Saylor, D. A., Schnülle, K., Sergeev, S. G., Siegel, M., Skielboe, A., Spencer, M., Starkey, D., Sung, H.-I., Teems, K. G., Turner, C. S., Uttley, P., Villforth, C., Weiss, Y., Woo, J.-H., Yan, H., Young, S. and Zu, Y. (2017) Space Telescope and Optical Reverberation Mapping Project. V. Optical spectroscopic campaign and emission-line analysis for NGC 5548. ApJ, 837(2), 131. https://doi.org/10.3847/1538-4357/aa5eb1.

Peterson, B. M. (1993) Reverberation mapping of active galactic nuclei. PASP, 105, 247–368. https://doi.org/10.1086/133140.

Peterson, B. M., Bentz, M. C., Desroches, L., Filippenko, A. V., Ho, L. C., Kaspi, S., Laor, A., Maoz, D., Moran, E. C., Pogge, R. W. and Quillen, A. C. (2005) Multiwavelength monitoring of the dwarf Seyfert 1 galaxy NGC 4395. I. A reverberation-based measurement of the black hole mass. ApJ, 632(2), 799–808. https://doi.org/10.1086/444494.

Peterson, B. M., Berlind, P., Bertram, R., Bischoff, K., Bochkarev, N. G., Borisov, N., Burenkov, A. N., Calkins, M., Carrasco, L., Chavushyan, V. H., Chornock, R., Dietrich, M., Doroshenko, V. T., Ezhkova, O. V., Filippenko, A. V., Gilbert, A. M., Huchra, J. P., Kollatschny, W., Leonard, D. C., Li, W., Lyuty, V. M., Malkov, Y. F., Matheson, T., Merkulova, N. I., Mikhailov, V. P., Modjaz, M., Onken, C. A., Pogge, R. W., Pronik, V. I., Qian, B., Romano, P., Sergeev, S. G., Sergeeva, E. A., Shapovalova, A. I., Spiridonova, O. I., Tao, J., Tokarz, S., Valdes, J. R., Vlasiuk, V. V., Wagner, R. M. and Wilkes, B. J. (2002) Steps toward determination of the size and structure of the broad-line region in active galactic nu-

clei. XVI. A 13 year study of spectral variability in NGC 5548. ApJ, 581(1), 197–204. https://doi.org/10.1086/344197.

Peterson, B. M., Ferrarese, L., Gilbert, K. M., Kaspi, S., Malkan, M. A., Maoz, D., Merritt, D., Netzer, H., Onken, C. A., Pogge, R. W., Vestergaard, M. and Wandel, A. (2004) Central masses and broad-line region sizes of active galactic nuclei. II. A homogeneous analysis of a large reverberation-mapping database. ApJ, 613(2), 682–699. https://doi.org/10.1086/423269.

Peterson, B. M., Grier, C. J., Horne, K., Pogge, R. W., Bentz, M. C., De Rosa, G., Denney, K. D., Martini, P., Sergeev, S. G., Kaspi, S., Minezaki, T., Zu, Y., Kochanek, C. S., Siverd, R. J., Shappee, B., Araya Salvo, C., Beatty, T. G., Bird, J. C., Bord, D. J., Borman, G. A., Che, X., Chen, C. T., Cohen, S. A., Dietrich, M., Doroshenko, V. T., Drake, T., Efimov, Y. S., Free, N., Ginsburg, I., Henderson, C. B., King, A. L., Koshida, S., Mogren, K., Molina, M., Mosquera, A. M., Motohara, K., Nazarov, S. V., Okhmat, D. N., Pejcha, O., Rafter, S., Shields, J. C., Skowron, D. M., Skowron, J., Valluri, M., Van Saders, J. L. and Yoshii, Y. (2014) Reverberation mapping of the Seyfert 1 galaxy NGC 7469. ApJ, 795(2), 149. https://doi.org/10.1088/0004-637X/795/2/149.

Peterson, B. M., Wanders, I., Bertram, R., Hunley, J. F., Pogge, R. W. and Wagner, R. M. (1998) Optical continuum and emission-line variability of Seyfert 1 galaxies. ApJ, 501(1), 82–93. https://doi.org/10.1086/305813.

Rakshit, S. (2020) Broad line region and black hole mass of PKS 1510-089 from spectroscopic reverberation mapping. A&A, 642, A59. https://doi.org/10.1051/0004-6361/202038324.

Rakshit, S., Stalin, C. S. and Kotilainen, J. (2020) Spectral properties of quasars from Sloan Digital Sky Survey data release 14: The catalog. ApJS, 249(1), 17. https://doi.org/10.3847/1538-4365/ab99c5.

Rakshit, S., Woo, J.-H., Gallo, E. et al. (2019) The Seoul National University AGN monitoring project. II. BLR size and black hole mass of two AGNs. ApJ, 886(2), 93. https://doi.org/10.3847/1538-4357/ab49fd.

Reines, A. E., Greene, J. E. and Geha, M. (2013) Dwarf galaxies with optical signatures of active massive black holes. ApJ, 775, 116. https://doi.org/10.1088/0004-637X/775/2/116.

Sagar, R. (1999) Some new initiatives in optical astronomy at UPSO, Nainital. CSci, 77(5), 643–652. https://www.currentscience.ac.in/Volumes/77/05/0643.pdf.

Sagar, R., Omar, A., Kumar, B., Gopinathan, M., Pandey, S. B., Bangia, T., Pant, J., Shukla, V. and Yadava, S. (2011) The new 130-cm optical telescope at Devasthal, Nainital. CSci, 101(8), 1020–1023. https://www.currentscience.ac.in/Volumes/101/08/1020.pdf.

Schlegel, D. J., Finkbeiner, D. P. and Davis, M. (1998) Maps of dust infrared emission for use in estimation of reddening and cosmic microwave background radiation foregrounds. ApJ, 500(2), 525–553. https://doi.org/10.1086/305772.

Shen, Y., Hall, P. B., Horne, K., Zhu, G., McGreer, I., Simm, T., Trump, J. R., Kinemuchi, K., Brandt, W. N., Green, P. J., Grier, C. J., Guo, H., Ho, L. C., Homayouni, Y., Jiang, L., I-Hsiu Li, J., Morganson, E., Petitjean, P., Richards, G. T., Schneider, D. P., Starkey, D. A., Wang, S., Chambers, K., Kaiser, N., Kudritzki, R.-P., Magnier, E. and Waters, C. (2019) The Sloan Digital Sky Survey Reverberation Mapping project: Sample characterization. ApJS, 241, 34. https://doi.org/10.3847/1538-4365/ab074f.

Stetson, P. B. (1987) DAOPHOT: A computer program for crowded-field stellar photometry. PASP, 99, 191–222. https://doi.org/10.1086/131977.

Tody, D. (1986) The Iraf data reduction and analysis system. In Instrumentation in Astronomy VI, edited by Crawford, D. L., vol. 0627, pp. 733–748. International Society for Optics and Photonics, SPIE. https://doi.org/10.1117/12.968154.

Tody, D. (1993) IRAF in the nineties. In Astronomical Data Analysis Software and Systems II, edited by Hanisch, R. J., Brissenden, R. J. V. and Barnes, J., vol. 52 of *ASPC*, pp. 173–183. https://ui.adsabs.harvard.edu/abs/1993ASPC...52..173T.

Urry, C. M. and Padovani, P. (1995) Unified schemes for radio-loud active galactic nuclei. PASP, 107, 803–845. https://doi.org/10.1086/133630.

Williams, P. R., Pancoast, A., Treu, T., Brewer, B. J., Peterson, B. M., Barth, A. J., Malkan, M. A., Rosa, G. D., Horne, K., Kriss, G. A., Arav, N., Bentz, M. C., Cackett, E. M., Bontà, E. D., Dehghanian, M., Done, C., Ferland, G. J., Grier, C. J., Kaastra, J., Kara, E., Kochanek, C. S., Mathur, S., Mehdipour, M., Pogge, R. W., Proga, D., Vestergaard, M., Waters, T., Adams, S. M., Anderson, M. D., Arévalo, P., Beatty, T. G., Bennert, V. N., Bigley, A., Bisogni, S., Borman, G. A., Boroson, T. A., Bottorff, M. C., Brandt, W. N., Breeveld, A. A., Brotherton, M., Brown, J. E., Brown, J. S., Canalizo, G., Carini, M. T., Clubb, K. I., Comerford, J. M., Corsini, E. M., Crenshaw, D. M., Croft, S., Croxall, K. V., Deason, A. J., Lorenzo-Cáceres, A. D., Denney, K. D., Dietrich, M., Edelson, R., Efimova, N. V., Ely, J., Evans, P. A., Fausnaugh, M. M., Filippenko, A. V., Flatland, K., Fox, O. D., Gardner, E., Gates, E. L., Gehrels, N., Geier, S., Gelbord, J. M., Gonzalez, L., Gorjian, V., Greene, J. E., Grupe, D., Gupta, A., Hall, P. B., Henderson, C. B., Hicks, S., Holmbeck, E., Holoien, T. W.-S., Hutchison, T., Im, M., Jensen, J. J., Johnson, C. A., Joner, M. D., Jones, J., Kaspi, S., Kelly, P. L., Kennea, J. A., Kim, M., Kim, S., Kim, S. C., King, A., Klimanov, S. A., Knigge, C., Krongold, Y., Lau, M. W., Lee, J. C., Leonard, D. C., Li, M., Lira, P., Lochhaas, C., Ma, Z., MacInnis, F., Manne-Nicholas, E. R., Mauerhan, J. C., McGurk, R., McHardy, I. M., Montuori, C., Morelli, L., Mosquera, A., Mudd, D., Müller-Sánchez, F., Nazarov, S. V., Norris, R. P., Nousek, J. A., Nguyen, M. L., Ochner, P., Okhmat, D. N., Papadakis, I., Parks, J. R., Pei, L., Penny, M. T., Pizzella, A., Poleski, R., Pott, J.-U., Rafter, S. E., Rix, H.-W., Runnoe, J., Saylor, D. A., Schimoia, J. S., Scott, B., Sergeev, S. G., Shappee, B. J., Shivvers, I., Siegel, M., Simonian, G. V., Siviero, A., Skielboe, A., Somers, G., Spencer, M., Starkey, D., Stevens, D. J., Sung, H.-I., Tayar, J., Tejos, N., Turner, C. S., Uttley, P., Van Saders, J. ., Vaughan, S. A., Vican, L., Villanueva, S., Villforth, C., Weiss, Y., Woo, J.-H., Yan, H.,

Young, S., Yuk, H., Zheng, W., Zhu, W. and Zu, Y. (2020) Space Telescope and Optical Reverberation Mapping Project. XII. Broad-line region modeling of NGC 5548. ApJ, 902(1), 74. https://doi.org/10.3847/1538-4357/abbad7.

Williams, P. R., Treu, T., Dahle, H., Valenti, S., Abramson, L., Barth, A. J., Brewer, B. J., Dyrland, K., Gladders, M., Horne, K. and Sharon, K. (2021) Dynamical modeling of the C IV broad line region of the $z = 2.805$ multiply imaged quasar SDSS J2222+2745. ApJ, 915(1), L9. https://doi.org/10.3847/2041-8213/ac081b.

Woo, J.-H., Cho, H., Gallo, E., Hodges-Kluck, E., Le, H. A. N., Shin, J., Son, D. and Horst, J. C. (2019) A 10,000-solar-mass black hole in the nucleus of a bulgeless dwarf galaxy. NatAs, 3(8), 755–759. https://doi.org/10.1038/s41550-019-0790-3.

Woo, J. H., Yoon, Y., Park, S., Park, D. and Kim, S. C. (2015) The black hole mass-stellar velocity dispersion relation of narrow-line Seyfert 1 galaxies. ApJ, 801(1), 38. https://doi.org/10.1088/0004-637X/801/1/38.